The GIFTS Fast Model: Clouds, Aerosols and Surface Emissivity

James E. Davies, Hung-Lung Huang and Erik R. Olson
SSEC/CIMSS
University of Wisconsin - Madison
1225 West Dayton St.
Madison, WI 53706, U.S.A.

ABSTRACT
A cloud model that represents both liquid and ice phases has been incorporated into the GIFTS (Geostationary Infrared Fourier Transform Spectrometer) fast radiative transfer model (GIFTSFRTE). The cloud model is limited to a single cloud layer of either liquid water droplets or ice crystals and requires, as input, the ice crystal or liquid droplet effective diameter and optical depth. This information is provided by condensate profiles of effective diameter and mixing ratio from the MM5 mesoscale model. Verification of GIFTSFRTE is achieved through comparison with LBLRTM and DISORT. Discrepancies can be of the order of a few Kelvin compared to tenths of a Kelvin under cloud free conditions. Spectral variations in surface emissivity typical of bare soil also give rise to top-of-atmosphere brightness temperature variations of a few Kelvin, compared to a unit emissivity Earth surface, for cloud optical depths of one.

KEY WORDS
GIFTS, radiative transfer, fast model, clouds, surface emissivity

1 Introduction

The GIFTS (Geostationary Infrared Fourier Transform Spectrometer) fast radiative transfer model (GIFSTFRTE) [1], initially a clear sky model, is evolving to include the radiative effects of clouds, aerosols and surface spectral emissivity. The impetus for continued model development is to provide accurate and rapid computations of the infrared emission of the Earth's surface and atmosphere, at high spectral resolution, to serve the needs of algorithm developers working to retrieve geophysical quantities from hyperspectral satellite observations.

For GIFTS simulations, fast model input and output data are organized into data cubes. A data cube has dimensions 128 by 128 to correspond with the GIFTS sensor array, with a third dimension that contains atmospheric profile information (inputs) or spectral information (outputs). Fig. 1 shows the surface heights for a GIFTS data cube centered at approximately 34.51N, 86.82W. Rows and columns are defined to be on the interval [-64:64] with row 0 and column 0 unassigned. Each pixel is 4 km square.

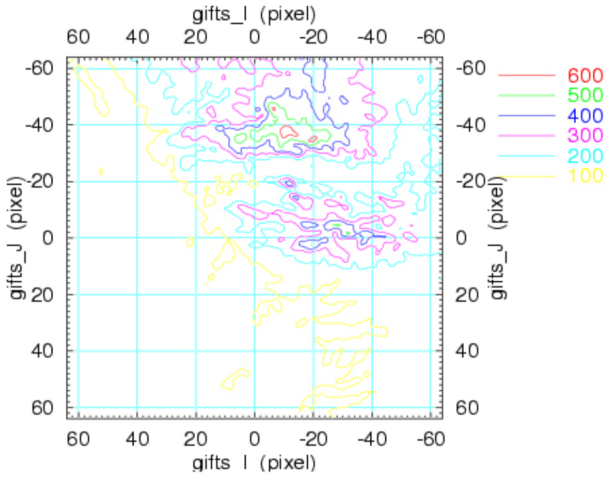

Figure 1: Surface height contour plot for an arbitrary GIFTS data cube. Rows and columns are defined to be on the interval [-64:64] with row 0 and column 0 unassigned.

Atmospheric profile data are represented as 312 floating-point values in a binary record; 16384 such records constitute a GIFTS atmospheric profile data cube. Atmospheric profile data are stored at the 101 pressure levels defined for AIRS (Atmospheric Infra-Red Sounder) profile retrievals. The first 303 values per record are ordered as 101 temperatures (K), 101 water vapor concentrations (g/kg) and 101 ozone concentrations (ppmv). The ordering is lowest pressure to highest pressure. The remaining 9 values are, in this order, liquid water path (g/m^2), ice water path (g/m^2), surface skin temperature (K), surface altitude (m), latitude (deg +N), longitude (deg +E), pressure level of liquid condensate (hPa), pressure level of ice condensate (hPa) and, finally, surface pressure (hPa). See Fig. 2.

2 Cloud model

Variations in the microphysical properties of clouds, in terms of the phase, size distribution, number density, and vertical distribution, make the inclusion of clouds into radiative transfer models troublesome. Yang [2] parameterized cloud optical properties into transmittance and reflectance functions with the aid of the well known multiple

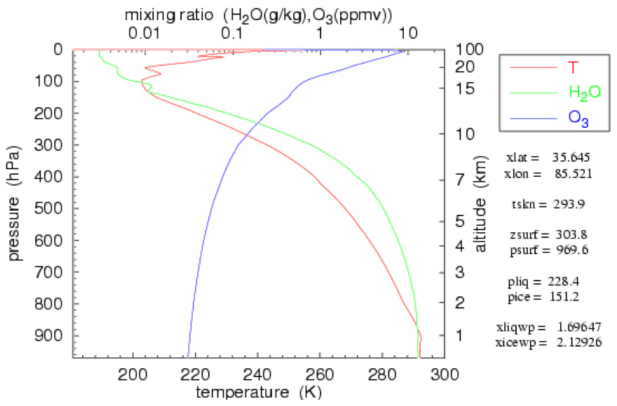

Figure 2: Cloudy atmospheric profile. The liquid water path (xliqwp) is 1.696 g/cm^2 and the ice water path (xicewp) is 1.129 g/cm^2. The surface skin temperature is 293.9 (K) and liquid and ice cloud cloud-top pressures are 228.4 and 151.2 hPa respectively. The cloud-top pressure is defined to be the lowest pressure at which a mass-in-mass mixing ratio of 1 x 10^{-6} is observed.

scattering code DISORT [3]. These computations were performed for both ice and liquid clouds (for a range of effective droplet diameters, cloud optical depths and observation zenith angles) at 201 wavenumbers covering the spectral range from 500 to 2500 wavenumbers. The resulting parameterized cloud transmittance and reflectance functions are coupled with a clear sky radiative transfer model to permit the rapid simulation of hyperspectral observations of top-of-atmosphere radiances in the presence of clouds.

Fig. 3 is a schematic to show the radiative approximation used in GIFTSFRTE. I is the top-of-atmosphere radiance and it is comprised of several parts, specfically,

$$I_0 = \varepsilon B(T_s)\frac{\tau_s}{\tau_c} + \int_{\tau_s}^{\tau_c} B(T(\tau))d\tau + (1-\varepsilon)I_0^{\downarrow}\frac{\tau_s}{\tau_c}\,, \quad (1)$$

$$I_0^{\downarrow} = \frac{\tau_s}{\tau_c}[I_1^{\downarrow}\mathbb{T}(\mu) + I_c(\mu)] + \int_{\tau_c}^{\tau_s} B(T(\tau))\frac{\tau_s}{\tau^2}\,d\tau\,, \quad (2)$$

$$I_c = [1 - \mathbb{R}(\mu) - \mathbb{T}(\mu)]B(T_c)\,, \quad (3)$$

$$I_1 = \int_{\tau_c}^{1} B(T(\tau))d\tau\,, \quad (4)$$

$$I_1 = \int_{\tau_c}^{1} B(T(\tau))d\tau\,. \quad (5)$$

In the preceding, ε is the surface emissivity, T_s is the surface temperature, B is the Planck function, $T(\tau)$ is the air temperature at transmittance τ, τ_s is the transmittance of the entire atmospheric column and τ_c is the transmittance down to the cloud top. The the cloud layer albedo and transmittance are denoted $\mathbb{R}$ and $\mathbb{T}$, respectively.

The cloud model accepts as input the effective diameter of cloud droplets, the cloud phase (liquid or ice), the visible optical thickness of the cloud and the pressure level

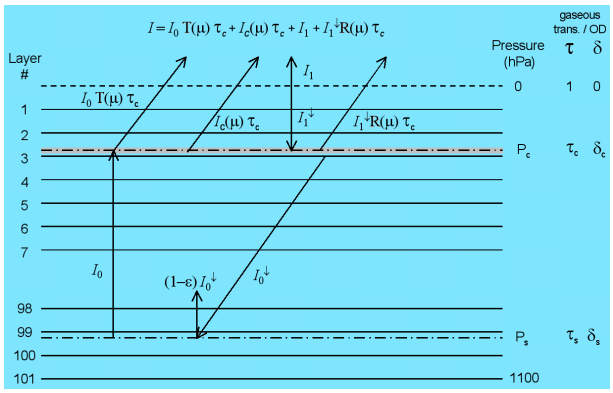

Figure 3: Radiative transfer approximation used in GIFTS fast model (GIFTSFRTE) for including cloud layer reflection & transmission and surface emissivity

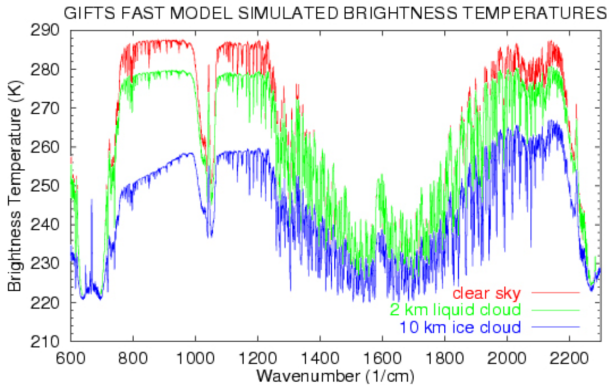

Figure 4: Fast model simulated spectra at GIFTS spectral resolution for clear sky, liquid cloud at 2 km altitude and ice cloud at 10 km altitude. The ice cloud is comprised of hexagonal ice crystals and the liquid cloud consists of spherical water droplets. In both cases the effective particle size is 40 mm and the optical depth is 2.

at the cloud top. GIFTSFRTE can accommodate a single cloud layer of either ice crystals or liquid water droplets. The mesoscale model MM5 [4] delivers concentrations and effective diameters of five condensate types (two liquid, three ice) at the 101 atmospheric levels. At present, only a single layer cloud of liquid or ice can be included so that a selection rule must be applied in the presence of mixed phase and multi-layer clouds. The selection rule invoked is that the cloud phase found at the highest altitude is the one included in model simulations. The optical depth is determined by the column amount of that phase but the effective diameter of particles is drawn from the condensate profile interpolated to the nominated cloud top pressure. Fig. 4 shows three spectra simulated by the fast model; for clear sky, for liquid cloud at 2 km altitude and for ice cloud at 10 km altitude.

3 Model Verification

To compute brightness temperatures for comparison with GIFTSFRTE we: (a) execute LBLRTM in optical depth mode to generate layer optical depths for a standard clear atmosphere (layers defined using the 101 AIRS pressure levels), (b) a cloud layer in terms of its altitude, type (i.e. liquid droplet or ice crystal habit) and moments of its size distribution, (c) execute LBLDIS [5] which combines the gaseous optical depths from LBLRTM [6] and cloud single scattering properties of the cloud layer and introduces them into DISORT, and (d) take the radiances generated by DISORT at some specified resolution and spectrally reduce them to GIFTS channels radiances finally converting to brightness temperature. For verification purposes, these brightness temperatures are considered "truth".

Fig. 5 shows, for the GIFTS long wave band, the difference between top-of-atmosphere brightness temperatures computed by LBLRTM and by DISORT (using LBLRTM generated layer optical depths) for a clear sky using different DISORT bandwidths. The comparisons show that, for LBLDIS executed with spectral step size 0.02 cm^{-1}, discrepencies of as large as 4 K occur in the CO_2 band centred at 15 μm and discrepencies of approximately 2 K occur in the 9.6 μm O_3 band. Reducing the spectral step size to 0.01 cm^{-1}, can reduce discrepencies to approximately 3 K in the CO_2 band and approximately 1 K in the O_3 band. In the window region between these major absorption features, LBLDIS under-estimates the brightness temperature by approximately 1 K. Reducing the spectral step size further to 0.001 cm^{-1} assists in removing brightness temperature difference fluctuations in the O_3 band but the magnitude of the discrepencies in the CO_2 band and the window region remain largely unchanged. It is thought that the reason for these discrepencies is in the formulation of effective layer optical depth, required by DISORT over a finite width bandpass. There is an implicit assumption that the illumination over a narrow bandpass is spectrally flat, an approximation which, for any given bandpass width, becomes increasingly poor with increasing altitude.

Since DISORT is only required up to the atmospheric level where clouds are present, this difficulty can be largely avoided by dividing the atmosphere into lower and upper sections. In the lower section, DISORT operates upon LBLRTM optical depths binned into 0.01 cm^{-1} averages. The upwelling radiances from the lower section are interpolated to the wavenumber scale of high spectral resolution LBLRTM transmittance mode calculations of the upper section. The radiance emergent at the top of the atmosphere is computed as,

$$I'_i = \mathrm{TRP}[\nu^*_i, N, \nu, I] \times \tau^*_i + I^*_i \quad , \qquad (6)$$

where I^*_i and τ^*_i are the monochromatic radiances and transmittances from LBLRTM at wavenumber ν^*_i. I and ν are the narrow bandpass radiances and transmittances from LBLDIS and TRP is a linear interpolation function [7]. By way of explanation, if X and Y are N element vectors (X monotonic), and if x is a scalar within the span of X, the statement $y = \mathrm{TRP}[x, N, X, Y]$ assigns to y the value $Y_i + \dfrac{x - X_i}{X_{i+1} - X_i}(Y_{i+1} - Y_i)$, where x falls between the elements X_i and X_{i+1}. Spectral reduction of I' to GIFTS channel radiances provides the simulated top-of-atmosphere radiances. In the implementation of Eqn. 6 we computed I from the surface (1013 hPa) to 103 hPa. I^*_i and τ^*_i are computed from 103 hPa to space with the lower boundary characterized by unit emissivity and absolute zero temperature.

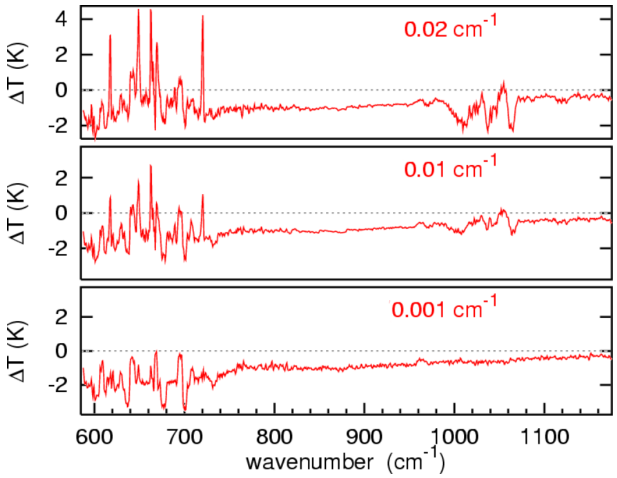

Figure 5: The difference in top-of-atmosphere brightness temperature computed by LBLRTM and by DISORT (using LBLRTM generated layer optical depths) for a clear sky standard atmosphere (US 1976) and for different DISORT bandwidths.

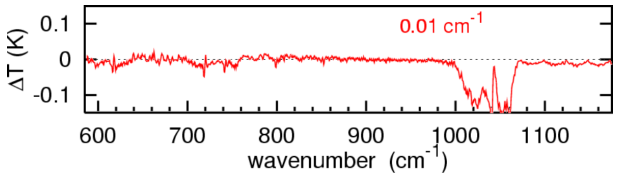

Figure 6: By dividing the atmosphere at 103 hPa, GIFTS channel brightness temperature differences are reduced to approximately 0.02 K over most of the GIFTS long wave band.

For the clear sky case, Fig. 6 shows that dividing the atmosphere at 103 hPa reduces GIFTS channel brightness temperature differences to approximately 0.02 K over most of the GIFTS long wave band. In the ozone band near 1050 cm^{-1} differences of approximately 0.1 K can still exist because of the abundance of ozone at stratospheric levels.

Verification of the accuracy of GIFTSFRTE under cloudy conditions consists of comparing top-of-atmosphere brightness temperatures computed by GIFTSFRTE with those from LBLDIS for certain idealised cloudy atmospheres. For the purposes of verification, the LBLDIS

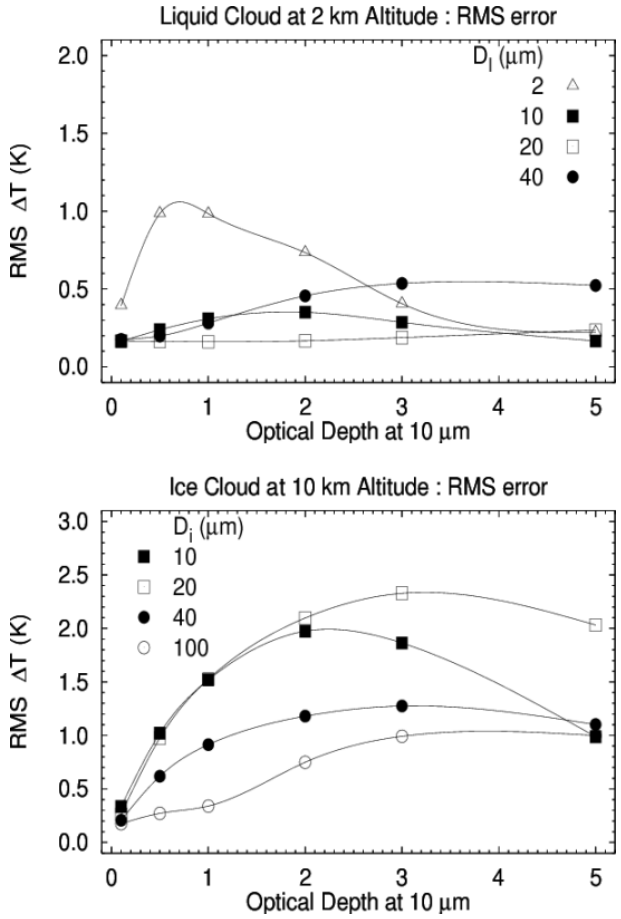

Figure 7: RMS difference between FAST and TRUTH brightness temperatures for liquid cloud with a cloud-top altitude of 2 km (upper panel) and for ice cloud with a cloud-top altitude of 10 km (lower panel).

results (obtained in the manner described above) are denoted TRUTH and the equivalent GIFTSFRTE results are denoted FAST. The atmospheres are idealized in the sense that for TRUTH, cloud droplets are confined to a single AIRS layer and are described by a mono-modal size distribution of variable mode radius but fixed width parameter. For FAST, the cloud layer is defined at the pressure level at the top of the TRUTH layer. Comparisons are made for liquid and ice clouds, each for four effective diameters and six optical depths. In each case the clear atmosphere profile, to which cloud properties are added, is the US 1976 standard atmosphere.

Fig. 7 shows the RMS difference between FAST and TRUTH brightness temperatures for the case of liquid cloud with a cloud-top altitude of 2 km and ice cloud with a cloud-top altitude of 10 km. The RMS differences are computed for GIFTS channel brightness temperatures over the wavenumber range 587 to 2350 cm^{-1}.

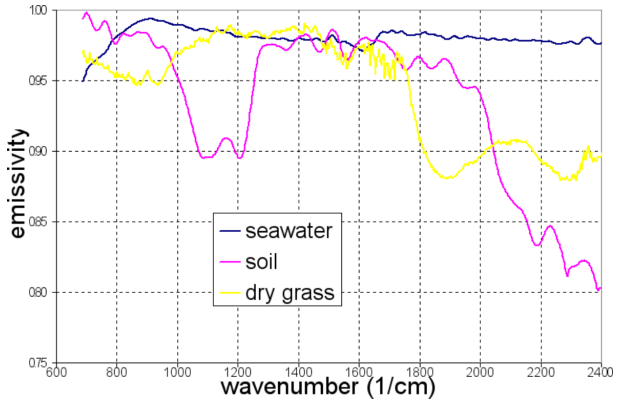

Figure 8: Spectral emissivity of seawater, soil and dry grass from the MODIS UCSB emissivity library.

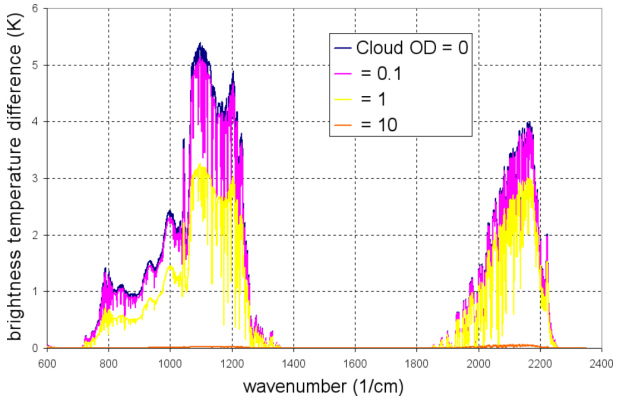

Figure 9: Difference in the simulated top-of-atmosphere brightness temperature for a soil surface and blackbody surface (blackbody less soil). The brightness temperature difference is shown for differing amounts of liquid water cloud at 500 hPa.

4 Surface Emissivity

Natural surfaces have emissivities that can be less than unity and vary spectrally. Fig. 8 shows some examples drawn from the MODIS UCSB emissivity library.

A difference arises in the simulated top-of-atmosphere brightness temperature when the Earth's surface, instead of being represented by a blackbody, is a natural surface. Fig. 9 shows the extent of this difference for a soil surface in the presence of differing amounts of liquid water cloud at 500 hPa. Where the surface emissivity deviates significantly from unity and, at the same time, the atmosphere is highly transmissive, top-of-atmosphere differences of several degrees can be observed even through clouds of unit optical depth. This makes clear the need for accurate characterization of surface properties if realistic top-of-atmosphere radiances are to be simulated over land.

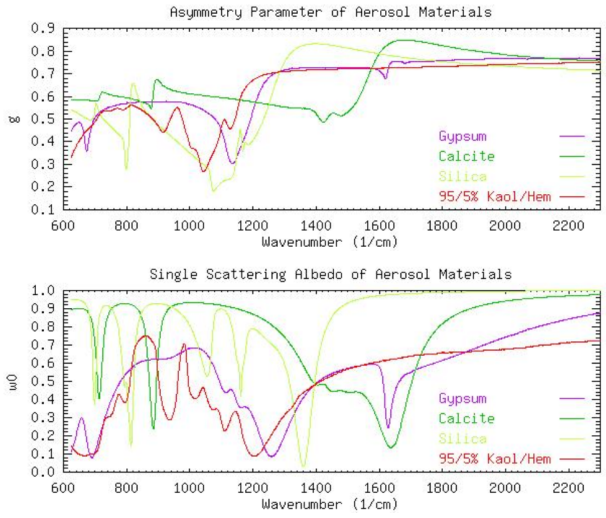

Figure 10: Assymetry parameter (upper panel) and single scattering albedo (lower panel) of radiatively important aerosol species [8].

5 Aerosol Effects

The presence of significant concentrations of atmospheric aerosol may have a measurable impact on top-of-atmosphere radiances over parts of the GIFTS spectrum. Through collaborations [8] four specific aerosol types have been identified for future inclusion into the GIFTS fast model. These are gypsum, calcite, silica and a mixture of kaolin and hematite, each with a specific size distribution. Fig. 10 shows the optical properties of these aerosol species derived, using Mie theory, from their spectral complex refractive indices. We are presently investigating ways to incorporate aerosol effects into GIFTSFRTE.

6 Conclusions and Further Work

A new liquid cloud and ice cloud model has been incorporated into the GIFTS fast radiative transfer model. The verification of this code against the more rigorously tested LBLRTM and DISORT shows that discrepancies on the scale of a few degrees Kelvin still exist. There also remain some significant issues with regard to forward modeling high spectral resolution radiances in the presence of mixed phase and multi-level cloud, and cloud which is vertically thick but optically thin. We are presently working on integrating the fast model with databases of surface spectral emissivity and models of radiatively important aerosol species. This work requires a commensurate effort in the development of verification methodologies that properly employ the best available radiative transfer models operating on identical base data.

This research is jointly supported by Navy MURI grant N00014-01-1-0850, NOAA GIFTS PAP grant NA07EC0676, and NASA GIFTS NAS1-00072.

References

[1] James E. Davies, Erik R. Olson, and Derek J. Posselt. Cloud model upgrade to the gifts fast radiative transfer model. Technical Report UW SSEC Publication No.03.09.D1, University of Wisconsin-Madison, Space Science and Engineering Center, 2003.

[2] Ping Yang. *A fast radiative transfer code for cirrus clouds and water clouds*. Department of Atmospheric Sciences, Texas A&M University, College Station, Texas 77843, December 2002.

[3] Knut Stamnes, S-Chee Tsay, Warren Wiscombe, and Kolf Jayaweera. Numerically stable algorithm for discrete–ordinate–method radiative transfer in multiple scattering and emitting layered media. *Applied Optics*, 27(12):2502–2509, 1988.

[4] G. A. Grell, J. Dudhia, and D. R. Stauffer. A description of the fifth-generation Penn State/NCAR mesoscale model (MM5). *NCAR Tech. Note TN-398+STR*, page 117 pp., 1994.

[5] Dave D. Turner. *Microphysical properties of single and mixed-phase Arctic clouds derived from ground-based AERI observations*. PhD thesis, University of Wisconsin - Madison, Madison, Wisconsin, 2003.

[6] Shepard A. Clough and Michael J. Iacono. Line-by-line calculations of atmospheric fluxes and cooling rates. 2: Applications to water vapor carbon dioxide, ozone, methane, nitrous oxide and the halocarbons. *Journal of Geophysical Research*, 100:16519–16535, 1995.

[7] Alfred M. Morris. *NSWC Library of Mathematics Subroutines*. Naval Surface Warfare Center, Silver Spring, MD, 1990.

[8] Irina Sokolik. Personal communication, 10^{th} November, 2003.